RSC Advances

ROYAL SOCIETY OF CHEMISTRY

www.rsc.org/advances

Methods to delay deactivation of zeolites on furan acylation: continuous liquid-phase technology and solvent effects

Yuannan Xiong[a,b], Wenqi Chen[a,b], Jianun Ma[a,b], Zhihua Chen[a,b], Aiwu Zeng[a,b*]

Abstracts: The continuous liquid-phase Friedel-Crafts acylation of furan with acetic anhydride was first carried out in a fixed-bed reactor over H-beta zeolite. A three-level, four-variable Box-Benkhen design combined with response surface methodology was employed to determine the optimal acylation conditions, and the accuracy of the models was verified by a validation experiments. In this study, it was found that lower liquid velocity and stronger polarity of the solvent were conducive to enhancing the catalytic activity and stability of H-beta zeolite. The reaction was limited by the acid sites poisoned due to the adsorption of the by-product and pore blockage. Moreover, the carbon deposit was proved to be the main reason for the deactivation of H-beta zeolite by using GC-MS, ^{13}C NMR MAS, ^{27}Al NMR MAS, TG/DTG and NH_3-TPD.

Keywords: Continuous liquid-phase; Acylation; Furan; Box-Benkhen design; Carbon deposit

1. Introduction

Friedel-Crafts acylation is a crucial method for synthesizing aromatic ketones, which are key intermediates in the production of valuable industrial and fine chemicals,[1-6] such as pharmaceuticals, insecticides, plasticizers, dyes and perfumes.[7,8] For example, furan can be converted into higher-value added products (2-acetylfuran) through Friedel-Crafts acylation reaction. It has been found that 2-acetylfuran mainly exists in fruit juices[9] and Maillard products from the thermal decomposition of glucose-1-phosphate.[10] As reported in the literatrues,[11-15] 2-acetylfuran is of considerable commercial importance due to its application in food additives and drug industries.

Traditionally, the Friedel-Crafts synthesis is carried out in liquid-phase by using Broensted acid (e.g. H_2SO_4, HCl and HF) or Lewis acids (e.g. $AlCl_3$, $FeCl_3$, and $TiCl_4$) as catalysts. However, the commonly encountered problems of such a synthesis include the disposal of spent catalysts, corrosion, toxicity and product isolation.[16] In line with more stringent environmental legislation, it is highly desirable to search for the ecofriendly and efficient heterogeneous catalysts such as zeolites,[17,18] heteropolyacids[19] or clays.[20] Compared with conventional liquid acids, zeolites have been proven to be the most potential catalyst for the industrial production of aromatic ketons in Friedel-Crafts type reaction due to their high thermal stability and environmentally friendly nature.[21] A recent important development in this field has been declared by Guignard,[22] which has established the first industrial and commercial application of zeolites for the acylation of anisole and veratrole with acetic anhydride. In case of furan, it is easy to undergo side reactions like polymerization, autoxidation, which results in a poor yield with traditional Friedel-Crafts acylation conditions.[23] Nevertheless, it should be pointed out that higher selectivities can be obtained by using zeolites as catalyst in the acylation of furan and aromatic ethers with acetic anhydride. After comparing the activities of HZSM-5, metal-modified HZSM-5, HY and Ce-Y

[a]Collaborative Innovation Center of Chemical Science and Engineering (Tianjin), State Key Laboratory of Chemical Engineering,
[b]Tianjin University, Institute of Chemical Engineering and Technology, Tianjin, 300072, People's Republic of China
[*]Corresponding author. Tel. +86-022-27404732. E-mail address: awzeng@tju.edu.cn

zeolites in the vapor phase acylation of furan, Reddy et al.[24] found that the maximum yield and the selectivity was obtained by HZSM-5 zeolite. Kantam et al.[7] studied liquid-phase Friedel-Crafts acylation of aromatics and heteroaromatics over beta zeolite, and the yield and selectivity of 2-acetylfuran were 40% and 88% respectively. Over H-beta zeolite, at milder reaction conditions and excess acetic anhydride, 2-acetylfuran was also selectively synthesized with a high yield of 91 mol%.[25] Whereas, zeolites are well known to be very sensitive to deactivation, especially when they are used as catalysts for acylation. Thus, it is urgent to re-examine the catalytic activity of zeolites in the acylation of furan with good stability and the best conditions. Besides, the research on its continuous liquid-phase technology has been scarcely reported.

In this work, the results had been obtained for the continuous liquid phase acylation of furan by acetic anhydride over H-beta zeolites. Optimization had also been done for the variables of affecting the yield of 2-acetylfuran, such as temperature, catalyst/furan weight ratio, anhydride/furan molar ratio and reaction time, by use of Response surface methodology (RSM) based on Box-Behnken design (BBD). Moreover, the effects of the liquid hourly space velocity (LVSH) and the polarity of the solvent on the catalytic performance were examined. The aim of this study is to explore the origin of deactivation of the zeolites. Deactivated zeolites were recovered and extracted in a soxhlet with dichloromethane. It is indicated that the organic compounds (coke) retained in the surface and channel of zeolites are responsible for the deactivation of zeolites through the analysis of GC-MS, ^{13}C NMR MAS, ^{27}Al NMR MAS, TG/DTG, and NH_3-TPD. This means that reaction processes is limited by the poisoning of the acid sites because of the adsorption of by-product and pore blockage, in coordination with the recent reports.[26-29]

2. Experimental

2.1 Materials

Furan (>99%) and tetraethyl ammonium hydroxide (TEAOH) were procured from Aladdin Reagent Co., Ltd. Acetic anhydride (98.5%) and acetic acid (99.5%) were supplied by Tianjin Jiangtian Chemical Technology Co., Ltd. 2-Acetylfuran (98.0%, GC) standard was provided by J&K Co., Ltd. The commercial aluminosilicate was purchased from Nankai University Catalyst Co., Ltd. All materials were used without further purification.

2.2 Catalyst preparation

H-beta zeolite was prepared according to the method reported by Matsukata et al..[30] The mixture of H-beta (10g), Al_2O_3 (3g) and 10 wt% nitric acid solution (4g) was stirred into homogeneous, then extruded it and cut into a short cylinder of 4 mm in length and 3 mm in diameter. The granular zeolites were dried at 120 °C for 2 h, and calcined at 550 °C for 5 h in a muffle furnace. In addition, zeolite samples were activated at 200°C under dry N_2 atmosphere for 2 h before catalytic experiments.

2.3 Catalyst characterization

X-ray diffraction (XRD) patterns were acquired on a Bruker D8-S4 diffractometer with Cu Kα radiation source, scanning from 4° to 30° (2θ) with scanning speed of 3°/min. The bulk Si/Al molar ratios of solid samples were determined by X-ray fluorescence (XRF) spectroscopy analysis

operating on a Bruker S4 Pioneer spectrometer. The Brunauer-Emmett-Teller (BET) surface area, total pore volume, pore size were measured on a Micrometrics Instrument Tristar 3000 surface area and pore analyzer.

Ammonia temperature-programmed desorption (NH_3-TPD) experiments were carried out on a TP-5079 instrument equipped with a thermal conductivity detector. The Surface acidity of zeolite H-beta was measured by the pyridine adsorption-desorption method using a Nicolet 750 infrared spectrometer coupled to a conventional high vacuum system. The sample was calcined at 450 ℃ for 120 min in an in situ IR gas cell under vacuum prior to pyridine adsorption. Then the temperature was cooled down to 90 ℃. Pyridine was adsorbed for 30 min and futher the physisorption pyridine was evacuated at 200 ℃ and 350 ℃ for 20 min respectively. The IR spectra were obtained at 200 ℃ and 350 ℃.

Thermogravimetric (TG) analysis was performed for the samples (10 mg) in the temperature range of 25-750 ℃ with a heating rate of 15 ℃/min under N_2 atmosphere, conducted on a PerkinElmer Diamond TG/DTA instrument. ^{13}C NMR and ^{27}Al NMR spectra were recorded using a Varian Infinity plus NMR (^{13}C, ^{27}Al 300 MHz) spectrometer in order to investigate the types of carbon deposit and the form of aluminum of zeolites. The scanning frequency was 75.4 MHz and pulse delay was 5.0 s. Chemical shifts (δ) were reported in ppm on behalf of the kind of carbon deposit and the form of aluminum respectively.

2.4 Reaction procedure

Response surface methodology (RSM) is a suitable tool to set up numerical models, to measure the influence of variables, and to determine the optimum process parameter. The most common designs, such as central composite design (CCD) and Box-Behnken design (BBD), of the principal response surface methodology have been widely used in various experiments. In this work, a three-level, four-variable Box-Benkhen design (BBD) was employed to design and analyze the effects of various reaction conditions on furan acylation, such as temperature (50-70 ℃), acetic anhydride/furan molar ratio (2-5), catalyst/furan weight ratio (0.232-0.464), and Time on stream (0.5-2.5 h) (data in Table S1 and S2 in Supporting Information). In a typical run, the mixture of furan (42 mmol), acetic anhydride (210 mmol) and zeolite catalyst (1 g) was introduced in a flask (50 ml) equipped with a cooler and a magnetic stirrer, and the mixture was allowed to heat up to 60 ℃ for 1.5 h.

The continuous experiments were carried out in a fixed-bed reactor (Fig. 1), consisting of a stainless steel tube (8 mm in diameter, 28 cm in length) with an electrical heater, which located in a vertical manner, and H-beta (5.7 g) zeolite samples were mounted in the middle isothermal region of the reactor. The catalyst was activated in situ at 200℃ under N_2 flow (100 ml/min) for 2 h before acylation reaction. Then the reaction emperature decreased to 60 ℃ and pressure was controlled at 0.6 MPa in N_2 flow (30 ml/min). Typically, the mixture of furan and acetic anhydride with a molar ratio of 1:5 was introduced at the top of the reactor by a metering pump (flow rate 0.1 ml/min). All liquid products were taken from the bottom of the reactor at regular intervals, and analyzed by using a gas chromatography (GC, Agilent 7890A) equipped with a flame ionization detector (FID) and DB-FFAP capillary column (30 m×0.25 mm×0.25 μm). The acylated products were also identified by mass spectroscopy (MS) equipped with a mass selective detector (MSD) (5975C inert MSD with Triple-Axis Detector (Agilent), details are documented in Supporting Information).

The molar yield (mol%) of 2-acetylfuran ($Y_{2\text{-ACF}}$) was calculated as follows:

$$Y_{2\text{-ACF}} = \frac{\%\text{mol (2ACF at time = t)}}{\%\text{mol (Furan at time = 0)}} \times 100 \quad (1)$$

3. Results and discussion

3.1 Characterization of H-beta zeolite

The framework Si/Al molar ratio of H-beta zeolite used in this work was 27.6. XRD pattern of the H-beta zeolite (Parent zeolite) is shown in Fig. 2. As can be seen, the characteristic diffraction peaks of the H-beta zeolite are at about 7.8° and 22.5° and the XRD crystallinity is almost 100%. The total surface area of the H-beta zeolite is 542 m^2/g (micropore surface area = 449 m^2/g, external surface area = 93 m^2/g) (calculated by the BET method), the total pore volume is 0.209 cm^3/g (measured by the t-plot method), and the average pore diameter is 0.56 nm (determined by Horvath–Kawazoe method). As recorded in Table 1, the information of Broensted and Lewis acid sites of H-beta zeolite can be acquired by the adsorption-desorption of pyridine followed by IR.

3.2 RSM experiments, analysis and optimization

The Box-Behnken design (BBD) and response values are shown in Table S1, S2 in Supporting Information. Among the various trials, the maximum yield of 2-acetylfuran is 87.6 mol% at trial #4 (condition: 70 °C, acetic anhydride/furan molar ratio=5, catalyst/furan weight ratio=0.348, 1.5 h). The effects of variables and their interactions which are significant on yield of 2-acetylfuran are shown in Fig. S2 (Supporting Information), indicating that the acetic anhydride/furan molar ratio (X_2) is the most significant factor affecting the molar yield of 2-acetylfuran. Besides, It suggests that the molar yield is considerably affected by those independent variables of temperature (X_1), catalyst/furan weight ratio (X_3), and time (X_4) as well as interaction terms of temperature and acetic anhydride/furan molar ratio (X_1X_2), catalyst/furan weight ratio and time (X_3X_4). It is also worth noticing that the regression coefficients of X_1, X_2, X_3 and X_4 are positive, and a high level of X_1, X_2, X_3 and X_4 contributes to 2-acetylfuran yield. However, the regression coefficients of X_1X_2, X_3X_4, X_2^2, X_3^2 and X_4^2 are negative, which results in the opposite effects. Further analysis on the results implies that a second-degree polynomial model is appropriate for the regression of acylation variables. The second-degree polynomial Eq. (2) (in coded values) is given below:

$$\begin{aligned} Y = {} & 73.31 + 8.60X_1 + 14.07X_2 + 9.85X_3 + 6.15X_4 - 2.98X_1X_2 \\ & - 3.45X_3X_4 - 4.54X_2^2 - 3.62X_3^2 - 3.32X_4^2 \end{aligned} \quad (2)$$

where Y is the predicted response of molar yield of 2-acetylfuran, X_i is the coded value of each variable (details in Eq.S1-S2 in Supporting Information). It must be pointed out that 2-acetylfuran was high selectively (approximately 100%) formed in the acylation of furan with acetic anhydride over H-beta zeolite. So the selectivity of 2-acetylfuran would not be taken as the response values.

Detail analysis of this model is presented in Table S3, S4 and Fig. S3-S4 (Supporting Information). The maximum yield of 2-acetylfuran (92.6 mol%) was obtained at the following

optimal conditions: 67 °C, acetic anhydride/furan molar ratio=4.99, catalyst/furan=0.42, and 2 h (Fig. S3 in Supporting Information). The results investigatied in this work are better than the previous reports,[31,32] which are summarized in Table 2. To confirm these results, three groups of verify experiments were carried out under optimum conditions. As expected, the output results from the model indicate a good agreement between the experimental and predicted values in Table 3. The actual 2-acetylfuran yield can reach 88.8 mol% under the aforementioned optimal conditions (No.3 in Table 3), which is close to the predicted value (92.6 mol%). Similar conclusion is given in two other groups (No.1 and No.2 in Table 3) with actual yield of 85.0 mol% and 87.4 mol% respectively. Thus, the result acquired from BBD confirms that the predicted model is accurate and reliable.

3.3 Continuous liquid-phase acylation experiments

Continuous liquid-phase acylation of furan with acetic anhydride over H-beta zeolite was carried out in a fixed bed reactor. Considering the fact that furan is quite labile and apt to polymerize, We adopt the second set of optimum acylation condition, which is set as follows: temperature=60 °C, acetic anhydride/furan molar=5, liquid hourly space velocity (LHSV, volume of reaction mixture introduced per volume of catalyst per hour) =0.667 h^{-1} (residence time=1.5 h), reaction pressure =0.6 MPa and catalytic amount =5.7 g. The reaction conditions and relevant results are presented in Table 4. As depicted in Fig. 3, The yield of 2-acetylfuran is plotted as a function of time on stream. The maximum yield of 2-acetylfuran and running time under the the LHSV of 0.435 h^{-1} are 79.7 mol % and 92.7 h respectively. The effect of the LVSH on acylation result was investigated, and the lower LVSH of 0.435 h^{-1} is conducive to enhancing activity and stability of H-beta zeolite than the LHSV of 0.667 h^{-1}, 0.855 h^{-1}. Thus, it is speculated that continuous flow of reagents can remove the ketone products from the acid sites of the zeolite, which significantly contributes to enhancing it's performance. Besides, compared with vapor-phase reactions, [24]this reaction system is more moderate and suitable for acylation of furan, and a higher yield and selectivity of 2-acetylfuran were obtained. However, the deactivation of H-beta zeolite was still obvious, and 2-acetylfuran remained absorbed, which made it more difficult for the diffusion of reactants from the interior channel of the catalyst. In addition, 2-acetylfuran would further react to form a larger by-product, and similar deactivation phenomenon was observed under the other LHSV.

3.4 Reasons for deactivation of zeolites

From what we have observed, we can summarize that a marked deactivation of H-beta zeolites occurs in the Friedel-Crafts acylation of furan with acetic anhydride. In order to find out the reasons of deactivation of catalyst, the analytical methods of the TG/DTG, GC-MS, ^{13}C MAS NMR, ^{27}Al MAS NMR, and NH_3-TPD were taken.

The thermogravimetric (TG) analysis was employed to investigate the amount of carbon deposit in the surface and pore of zeolites. For clarity, the corresponding DTG curves (the differential TG curve) for the parent and deactivated zeolites was also obtained. As presented in Fig. 4, both the parent and deactivated zeolite have a peak of weight loss in the range of 50-180 °C, respectively, which are mainly caused by the removal of adsorbed or more labile water in outer spheres. As for the deactivated zeolite, it also includes the desorption of residual organic materials of low molecular weight. In contrast, there is no weight loss for the parent zeolite over 180 °C, but

the peaks of weight loss exists in the range of 180-300 °C and 300-450 °C for the deactivated zeolite. At the range of 180-300 °C, the peak of deactivated zeolite directly coordinates to the desorption of strong polar product (2-acetylfuran), while at the range of 300-450 °C, the peak represents the removal of oligomers (poly 2-acetylfuran). It is obvious that 2-acetylfuran was adsorbed in the zeolite pores and can undergo a number of consecutive reactions that produce bulkier molecules which cannot diffuse out of the zeolite. In order to recover the organic compounds on the external and in the channel of the deactivated zeolite, the zeolite was treated with soxhlet extraction for 8 h using dichloromethane as solvent. After evaporation, the remaining organic components were analyzed by GC-MS. As expected, the acylated product was adsorbed on the acid sites due to its higher polarity, and consequently the adsorbed 2-acetylfuran can further react, giving larger by-product (Fig. 5). Still worse, the adsorbed bulkier molecules not only block the acid sites but also produce cokes with corresponding loss of catalytic activity.

The ^{13}C MAS NMR technique was employed to get a better insight into the origins of deactivation, which are similar to those reported in our previous work[33-34]. As shown in Fig. 6, the ^{13}C MAS NMR spectra of the deactivated and parent zeolite are given. In contrast to parent zeolite，the spectral features of deactivated zeolite is assigned to the presence of carbonaceous residues, which mainly composed by fat carbon, olefin carbon, aromatic carbon and poly aromatic carbon, etc. The fat hydrocarbon is closely correlated with band at 10-40 ppm[35], the band at 125-170 ppm has been mostly associated with aromatic carbon, while the band at 170-200 ppm is the characteristic signal of poly aromatic. For the deactivated zeolites investigated in our work , the carbon deposit consisting of fat hydrocarbon, aromatic carbon and aromatic oligomers in the channel and surface of catalyst is very serious. Two tall narrow bands at 10-40 and 170-200 ppm in coordination with fat hydrocarbon, aromatic carbon respectively, as well as a low broad band at 125-170 ppm represents poly aromatic. However, it is difficult to obtain accurate coke content by ^{13}C MAS NMR spectra.

It is highlighted that a correlation between the framework Si/Al molar ratio and the performances of H-beta zeolite. The influence of carbon deposit on zeolites framework can be characterized by ^{27}Al MAS NMR. In Fig. 7, the state of aluminum framework changes when the zeolite channel is filled with carbon deposit. There are two peaks corresponding to octahedral and tetrahedral Al sites in the range of -10-40 and 40-80 ppm [35], respectively. Compared with the parent sample, the tetrahedral Al concentration markedly decreased by roughly 50% on the deactivated zeolite due to the dealumination, while the octahedral Al concentration keeps constant. It is clear that the dealumination should be ascribed to the carbon deposit. Moreover, the tetrahedral Al represents Broensted acid sites, while the octahedral Al is on behalf of Lewis acid sites. Therefore, Fig. 7 may suggest that the Broensted acid is responsible for the Friedel-Crafts acylation reaction of furan with acetic anhydride.

NH_3-TPD analysis was taken to detect the number and types of acidic sites on the surface of zeolite samples by the measurement of the amounts of NH_3 desorbed at different temperatures. Ghiaci et al. [36] reported that the peaks at the range of 150-200 °C were assigned to weakly acidic sites and the peak located approximately at 400 °C to moderately-strong acidic sites. As depicted in Fig. 8, the NH_3-TPD profile of deactivated zeolite shows that the amount of acid sites of decreases sharply, especially for the moderately-strong acid sites, compared to the parent zeolite catalyst. It is demonstrated that an appropriate amount of moderately-strong acidic sites are conducive to enhancing the behavior of H-beta zeolite, in agreement with those recent report.[37,38]

3.5 Solvent effects

To delay the deactivation of the catalyst further, nitromethane and 1,2-dichloroethane are often used as solvents in this acylation reaction. Dimroth et al.[39] regarded solvents as structured isotropic continuum composed of individual solvent molecules with their own solvent/solvent interactions, and took into account specific solute/solvent interactions such as hydrogen-bonding and EPD/EPA interactions. Thus, $E_T(30)$ and normalized values E_T^N, the empirical parameters of solvent polarity were proposed. As shown in Fig.9, the yield of 2-acetylfuran increases relatively in the presence of nitromethane (E_T^N=0.481) but decreased relatively in 1,2-dichloroethane (E_T^N =0.327), compared to the absence of solvent. That is to say, the deactivation of H-beta zeolite will be delayed in the presence of nitromethane to some extent. Takeshi at al.[40] drew a conclusion that stronger polar nitromethane (E_T^N=0.481) can promote the desorption of 2-acetylfuran formed in the micropores of H-beta zeolite. Meanwhile, weaker polar 1,2-dichloroethane (E_T^N =0.327) can't promote the desorption process, but also may block the generation of acyl cation due to the dilution effect of solvent. However, it was also mentioned by Moreau et al.[41] that an increase in the solvent polarity may lead to competitive adsorption on the active sites among the solvents and reactants. Therefore, the correct selection of solvent is paramount to accelerate acylation reaction process. For prolonging its lifetime, it is indispensable to find out appropriate solvents to minimize the deactivation of catalyst.

4. Conclusions

The Response surface methodology (RSM) using Box-Behnken design (BBD) were successfully applied to analyze and optimize the experimental conditions. The results show a good fit to the model, and acetic anhydride/furan molar ratio is the most significant factors affecting the yield of 2-acetylfuran. Continuous liquid-phase acylation reaction of furan with acetic anhydride was first investigated in a fixed-bed reactor with a high yield of 92.6 mol% and selectivity of 100%. It is clearly verified that the polarity of solvent play important roles in improving catalytic stability. Stronger polar nitromethane can promote the desorption of 2-acetylfuran, thereby enhancing performance of catalyst. After the acylation reaction, the organic compounds retained on zeolites were recovered with soxhlet extraction and analyzed by GC-MS. TG/DTG, ^{13}C MAS NMR, ^{27}Al MAS NMR, NH_3-TPD. the analysis results confirm that the coke deposits are mainly due to the adsorption of by-product on acid sites and pore blockage, accounting for the deactivation of zeolites. The decrease of octahedral Al contributes to the deactivation of H-beta zeolite was observed by ^{27}Al MAS NMR. Moreover, the NH_3-TPD profiles show that the appropriate amount of moderately-strong acid sites are key to maintain the activity and stability of catalysts.

References

[1] M. Bejblova, D. Prochazkova and J. Cejka, *ChemSusChem*., 2009, **2**,486-499.

[2] J.A. Melero, R. V. Grieken, G. Morales and V. Nuno, *Catal. Commun.*, 2004, **5**, 131.

[3] I. Komoto, J.I. Matsuo and S. Kobayashi, *Top. Catal.*, 2002, **19**, 43.

[4] H. K. Heinichen and W. F. Holderich, *J. Catal.*, 1999, **185**, 408-414.

[5] P. Moreau, A. Finiels, P. Meric and F. Fajula, *Catal. Lett.*, 2003, **85**, 199-203.

[6] E. Fromentin, J. M. Coustard and M. Guisnet, *J. Mol. Catal. A: Chem.*, 2000, **159**, 377-388.

[7] M.L. Kantam, K.V.S. Ranganath, M. Sateesh, K. B. S. Kumar and B. M. Choudary, *J. Mol. Catal. A: Chem.*, 2005, **225**, 15-20.

[8] U. Freese, F. Heinrich and F. Roessner, *Catal. Today.*, 1999, **49**, 237-244.

[9] J. P. Yuan and F. Cheng, *J. Agric. Food Chem.*, 1998, **46**, 1286-1291.

[10] V.A. Yaylayan, D. Michiels and L. Istasse, *J. Agric. Food Chem.*, 2003, **51**, 3358-3366.

[11] R.G. Buttery, G.R. Teranishi, L.C. Ling and J.G. Turnbaugh, *J. Agric. Food Chem.*, 1990, **38**, 336-340.

[12] R.G. Buttery, G.R. Takeoka and L.C. Ling, *J. Agric. Food Chem.*, 1995, **43**, 1638-1640.

[13] M. Sakho, J. Crouzet and S. Seck, *J. Food Sci.*, 1985, **50**, 548-550.

[14] C. Bertez, M. Miouel, C. Coquelet, D. Sincholle and C. Bonne, *Biochem. Pharmacol*., 1984, **33**, 1757-1762.

[15] H. Flores, E.A. Camarillo and J. Mentado, *Thermochimica Acta.*, 2009, **493**, 76-79.

[16] G. Sartori and R, Maggi, *Chem. Rev.*, 2011, **111**, 181-214.

[17] K.G. Bhattacharyya, A.K. Talukdar, P. Das and S. Sivasanker, *Catal. Commun.*, 2001, **2**, 105-111

[18] Y. Sun and R. Prins, *Appl. Catal. A: Gen.*, 2008, **336**, 11-16.

[19] J. Kaur, K. Griffin, B. Harrison and I.V. Kozhevnikov, J. Catal., 2002, **208**, 448-455.

[20] G. D. Yadav, N.S. Asthana and V.S. Kamble, *Appl. Catal. A: Gen.*, 2003, **240**, 53-69.

[21] C. Guignard, V. Pedron, F. Richard, R. Jacquot, M. Spagnol, J. M. Coutard and G. Perot, *Appl. Catal. A: Gen.*, 2002, **234**, 79-90.

[22] M. Opietnik, A. Jungbauer, K. Mereiter and T. Rosenau, *Curr. Org. Chem.*, 2012, **16**, 2739-2744.

[23] P.R. Reddy, M. Subrahmanyam and S.J. Kulkarni, *Catal. Lett.*, 1998, **54**, 95-100.

[24] D. Rohan, C. Canaff, P. Magnoux and M. Guisnet, *J. Mol. Catal. A: Chem.*, 1998, **129**, 69-78.

[25] V.F.D. Álvaro, A.F. Brigas, E.G. Derouane, J.P. Lourenco and B.S. Santos, *J. Mol. Catal. Chem.* 2009, **305**, 100-103.

[26] P. Botella, A. Corma, J. M. LÓpez-Niteo, S. Valencia and R. Jacquot, *J. Catal.*, 2000, **195**, 161-168.

[27] K.M. Su, Z.H. Li, B.W. Cheng, L.Zhang, M.L. Zhang, and J.Ming, *Fuel Process.Technol.*, 2011, **92**, 2011-2015.

[28] H. S. Cerquira, P. Ayrault, J. Datka and M. Guisnet, *Microporous Mesoporous Mater*, 2000, **38,** 197.

[29] M. Matsukata, M. Ogura, T. Osaki, P. R. H. P. Rao, M. Nomura and E. Kikuchi, *Top. Catal.*, 1999, **9**, 77-92.

[30] C. J. Chapman, C. G. Frost and J. P. Hartley, *Tetrahedron Lett*., 2001, **42**, 773.

[31] I. Komoto, J. Matsuo and S. Kobayashi, *Top. Catal.*, 2002, **19**, 43.

[32] F. He, H. Wu and J. Chen, *Synth. Commun.*, 2008, **38**, 255.
[33] Z. H. Chen, Y. F. Feng, T. X. Tong and A. W. Zeng, *Appl. Catal. A: Gen.*, 2014, **482**, 92-98.
[34] Z. H. Chen, W. Q. Chen, T. X. Tong and A. W. Zeng, *J. Mol. Catal. A: Chem*., 2015, **396**, 231-238.
[35] P. Dejaifve, A. Auroux, P.C. Gravelle, J.C. Vedrine, Z. Gabelica and E.G. Derouane, *J.Catal.* 1981,**70**,123-136.
[36] M. Ghiaci, A. Abbaspur, R. Kia, C. Belver, R. Trujillano, V. Rives and M. A. Vicente, *Catal. Commun.*, 2007, **8**, 49-56.
[37] R. Srivastava, N. Iwasa, S.I. Fujita and M. Arai, *Catal. Lett.* 2009,**130**, 655-663.
[38] G.Y. Bai, J. Han, H.H. Zhang, C. Liu, X.W. Lan, F. Tian, Z.Zhao, and H. Jin, *RSC Adv.*, 2014, **4**, 27116-27121.
[39] V. K. Dimroth, C. Reichardt, T. Siepmann and F. Bohlmann, *Liebigs Ann. Chem.,* 1963, **661**, 1-37.
[40] T. Takeashi, T. Kai and E. Nakao, *Appl Catal A: Gen.*, 2004, **262**, 137.
[41] P. Moreau, A. Finiels, P. Meric and F. Fajula, *Catal. Lett.*, 2003, **85**, 199-203.

Figure Captions

Fig. 1. Continuous liquid-phase acylation of furan in fixed bed reactor apparatus diagram

Fig. 2. XRD patterns of the H-beta zeolites..

Fig. 3. 2-Acetylfuran yield (mol%) vs time as a function of the LHSV during continuous acylation of furan with acetic anhydride over H-beta zeolite in a fixed bed reactor. Experimental conditions: 60 °C; acetic anhydride/furan molar=5; reaction pressure=0.6 MPa; catalytic amount=5.7 g.

Fig. 4. TG/DTG curves of the parent and deactivated zeolite samples.

Fig. 5. Second acylation production, E-2,2'-(ethene-1,2-diyl)bis[2-furan].

Fig. 6. ^{13}C MAS NMR patterns of the the parent and deactivated zeolite samples.

Fig. 7. ^{27}Al MAS NMR patterns of the parent and deactivated zeolite samples.

Fig. 8. NH_3-TPD profiles of the parent and deactivated zeolite samples.

Fig. 9. 2-Acetylfuran yield (mol%) vs time in the presence and absence of solvent during continuous acylation of furan with acetic anhydride over H-beta zeolite in a fixed bed reactor. Experimental conditions: 60 °C; acetic anhydride/furan molar=5; LHSV=0.66 h^{-1}; reaction pressure=0.6 MPa; catalytic amount=5.7 g.

Table Captions

Table 1. Result of IR spectra of Py adsorbed on the zeolite H-beta at different desorption temperatures.

Table 2. The comparison results between literature and this work.

Table 3. Optimum conditions found by the model for the 2-acetylfuran yield.

Table 4. Continuous acylation reaction conditions and results.

Fig. 1

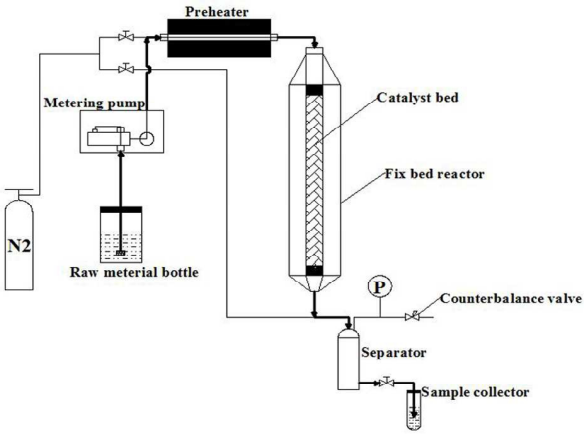

Fig 2.

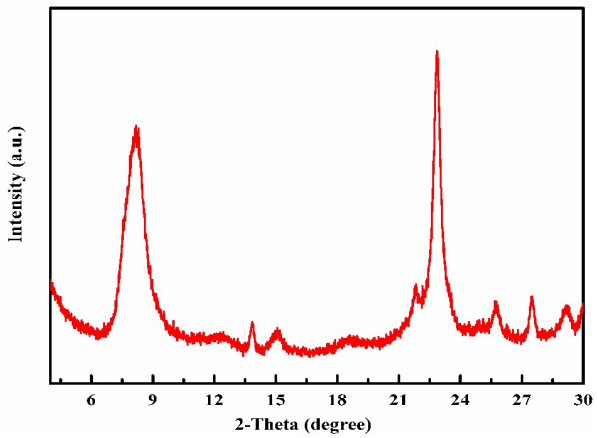

Fig. 3

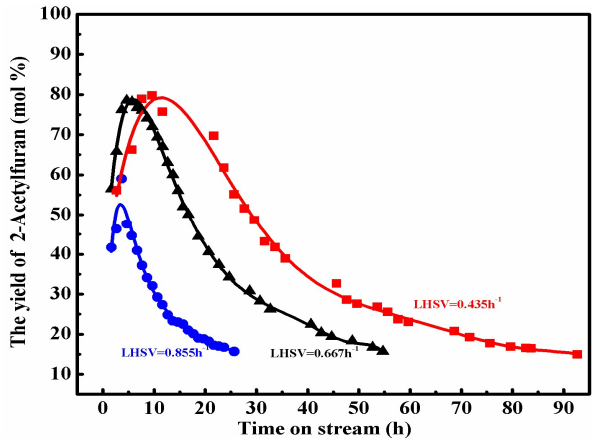

Fig. 4

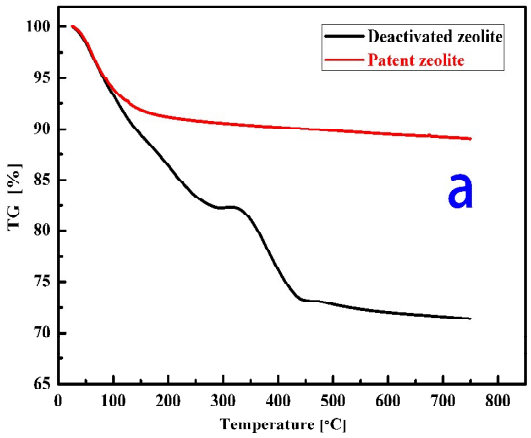

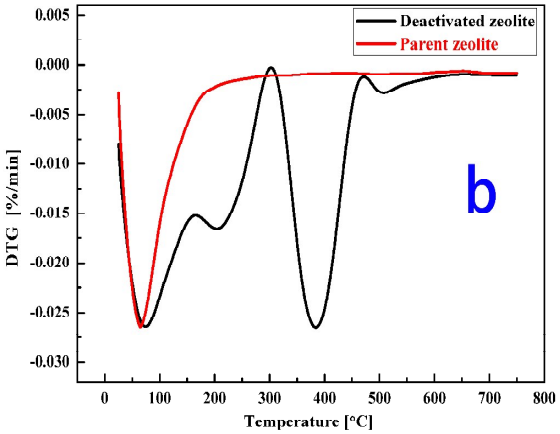

Fig. 5

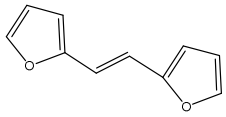

Fig. 6

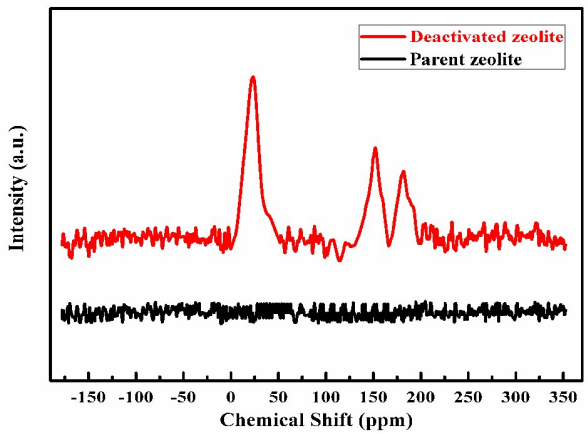

Fig. 7

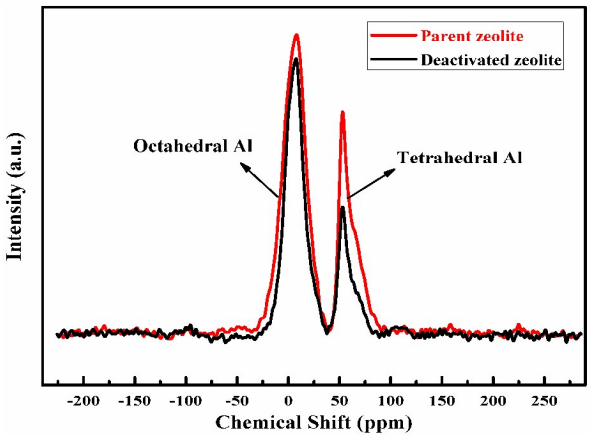

Fig. 8

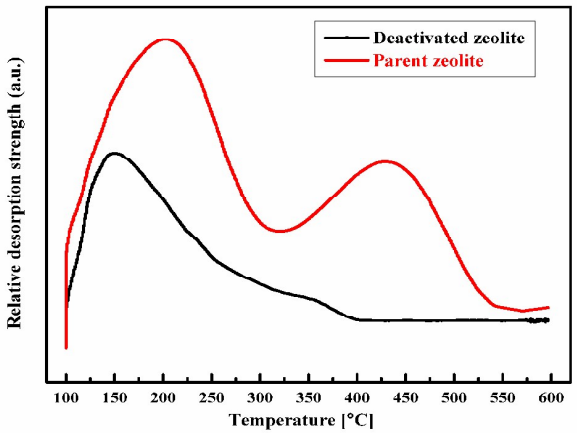

Fig. 9

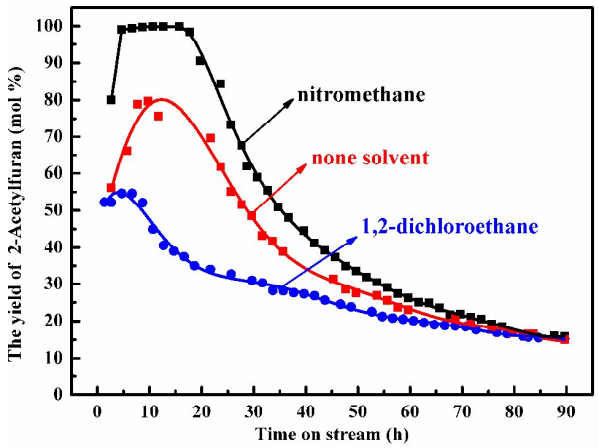

Table 1. Result of IR spectra of Py adsorbed on the zeolite H-beta at different desorption temperatures.

Sample	200°C			350°C		
	B acid	L acid site	B/C[A]	B acid	L acid site	B/C[a]
Parent zeolite	0.334	0.331	1.01	0.228	0.252	0.90

[a] B/C: the ration of B acid site to L acid site.

Table 2. The comparison results between literature and this work.

Literature	Catalyst	Catalyst/furan	Temperature (°C)	Furan/Acetic anhydride	Time/h	Solvent	Solvent/reactants	Y^A/mol%	X^B/%	S^C/%
1989[24]	Ce-B-Zeolite		200						23	99
	HZSM-5(19.7)				3			22.9(37.0)	44.1	83.9
	HZSM-5(30)				2			41.7(67.5)	93.0	72.0
	HZSM-5(280)				2			38.8(62.8)	94.2	66.6
1998[25]	CeZSM-5(30)		150	1:	3			29.7(48.0)	65.0	73.8
	LaZSM-5(30)				2			32.0(51.8)	85.8	60.5
	HY				2			13.4(21.6)	58.3	37.0
	CeHY				1			18.6(30.0)	48.8	60.4
2001[38]	$In(OTf)_3$+$LiClO_4$		ambient temperature			nitromethane		61.2(99)		
2002[39]	$AlCl_3$ $ZnCl_2$ $SnCl_2$ $Sn(OTf)_2$	30.6wt%(5mol%)	ambient temperature	1:2	4	nitromethane	411wt%(1.8ml)	2.5(4) 37.7(61) 31.5(51) 53.(86)		
2005[7]	Beta-I Beta-II	73.5wt%(0.5g)	40 25	1:2	8 12	1,2-dichloroethane	463wt%(10ml)		40 26	88 100
2008[40]	$Zn(OTf)_2 \cdot 6H2O$	10mol%	ambient temperature	1:1.5	4	nitromethane		46.4(75)		
2009[26]	Beta	28wt%	60	1:5	0.172			43.3(70) 56.3(91)		
This work	H-beta	46wt% 42wt%	60 67	1:5 1:5	1.5 2.1			87.4(141) 88.8(144)	99.8 100	100 100

[A] Y: the molar yield of 2-Acetylfuran, which followed by reduced mass yield presented in bracket.

[B] X: the conversion of furan.

[C] S: the selectivity of 2-acetylfuran.

Table 3 Optimum conditions found by the model for the 2-acetylfuran yield

Trials	Temperature (°C)	Acetic anhydride/furan (mol ratio)	Catalyst/furan (wt ratio)	Time (h)	Predicted Yield (mol%)	Actual Yield (mol%)	Selectivity (%)
1	65	4.28	0.40	1.85	87.7	85.0	100
2	60	5.00	0.46	1.50	89.1	87.4	100
3	67	4.99	0.42	2.12	92.6	88.8	100

Table 4 Continuous acylation reaction conditions and results

Trials	Temperature (°C)	Acetic anhydride/furan（mol ratio）	LHSV[a] (h^{-1})	Catalyst amount (g)	Pressure (MPa)	Feed flow rate (ml/min)	Solvent	The amount of 2-acetylfuran of catalyst (g/g Catalyst)
1	60	5	0.66	5.7	0.6	0.15	None	4.60
2	60	5	0.86	5.7	0.6	0.2	None	1.86
3	60	5	0.43	5.7	0.6	0.1	None	5.68
4	60	5	0.43	5.7	0.6	0.1	Nitromethane	5.97
5	60	5	0.43	5.7	0.6	0.1	1,2-Dichloroethane	3.48

[a] LHSV= 60•Feed flow rate/Reaction volume, h^{-1}; Reaction volume=14 ml.

Graphical Abstract:

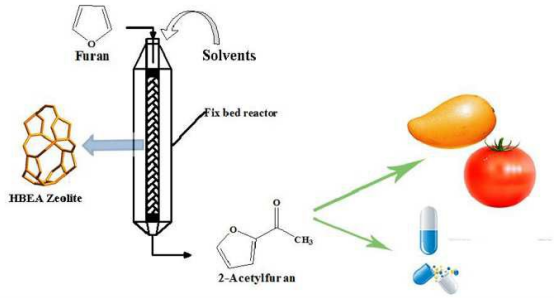

Friedel-Crafts acylation is a crucial method for synthesizing aromatic ketones, which are key intermediates in the production of valuable industrial and fine chemicals. For example, furan can be converted into higher-value added products (2-acetylfuran) through Friedel-Crafts acylation reaction. 2-acetylfuran is of considerable commercial importance due to its application in food additives and drug industries reported in previous work. The continuous liquid phase Friedel-Crafts acylation of furan with acetic anhydride over H-beta zeolite was first carried out in a fixed-bed reactor over H-beta zeolite. The optimal reaction conditions have been found by Response surface methodology (RSM) based on Box-Benkhen design. It was found that lower liquid velocity and stronger polarity of the solvent were conducive to enhancing the catalytic activity and stability of H-beta zeolite.